SymRK defines a common genetic basis for plant root endosymbioses with arbuscular mycorrhiza fungi, rhizobia, and *Frankia* bacteria

Hassen Gherbi*, Katharina Markmann†, Sergio Svistoonoff*, Joan Estevan*, Daphné Autran*, Gabor Giczey†, Florence Auguy*, Benjamin Péret*, Laurent Laplaze*, Claudine Franche*, Martin Parniske†, and Didier Bogusz*‡

*Equipe Rhizogenèse, Unité Mixte de Recherche Diversité et Adaptation des Plantes Cultivées (DIAPC), Institut de Recherche pour le Développement (IRD), 911 Avenue Agropolis, 34394 Montpellier Cedex 5, France; and †Department of Biology, Genetics, Ludwig-Maximilians-Universität, Maria-Ward-Strasse 1a, 80638 Munich, Germany

Root endosymbioses vitally contribute to plant nutrition and fitness worldwide. Nitrogen-fixing root nodulation, confined to four plant orders, encompasses two distinct types of associations, the interaction of legumes (Fabales) with rhizobia bacteria and actinorhizal symbioses, where the bacterial symbionts are actinomycetes of the genus *Frankia*. Although several genetic components of the host–symbiont interaction have been identified in legumes, the genetic basis of actinorhiza formation is unknown. Here, we show that the receptor-like kinase gene *SymRK*, which is required for nodulation in legumes, is also necessary for actinorhiza formation in the tree *Casuarina glauca.* This indicates that both types of nodulation symbiosis share genetic components. Like several other legume genes involved in the interaction with rhizobia, *SymRK* is also required for the interaction with arbuscular mycorrhiza (AM) fungi. We show that *SymRK* is involved in AM formation in *C. glauca* as well and can restore both nodulation and AM symbioses in a *Lotus japonicus symrk* mutant. Taken together, our results demonstrate that *SymRK* functions as a vital component of the genetic basis for both plant–fungal and plant–bacterial endosymbioses and is conserved between legumes and actinorhiza-forming Fagales.

actinorhizal symbioses | *Casuarina glauca* | mycorrhizae | signaling

Root endosymbioses are associations between plants and soil microorganisms involving intracellular accommodation of microbes within host cells. The most widespread of these associations is arbuscular mycorrhiza (AM), which is formed by the majority of land plants with fungi belonging to the phylum Glomeromycota (1). In contrast, nitrogen-fixing nodulation symbioses of plant roots and bacteria are restricted to four orders of eurosid dicots (2). Actinorhiza, formed by members of the Fagales, Rosales, and Cucurbitales with Gram-positive *Frankia* bacteria, differs from the interaction of legumes with Gram-negative rhizobia in several morphological and cytological aspects (3). Although these differences suggest independent regulatory mechanisms, the close relatedness of nodulating lineages indicates a common evolutionary basis of root nodulation symbioses (2). In the legume–rhizobia interaction, among the key factors mediating recognition between the plant and the bacteria are Nod factors (NFs). NFs are bacterial lipochitooligosaccharides with an *N*-acetylglucosamine backbone (4). The perception of NFs induces a series of responses in host roots, including ion flux changes and membrane depolarization, rhythmic calcium oscillations in and around the nucleus (calcium spiking), cytoskeletal modifications and root hair curling, and activation of cortical cell divisions (5). Extensive mutant screenings performed in legumes led to the identification of several loci involved in this signaling cascade, and recently most of the corresponding genes were identified by map-based approaches (6). In *Lotus japonicus*, two genes, *NFR1* and *NFR5* encoding receptor-like serine/threonine kinases with LysM domains, are assumed to be involved in NF perception, because the corresponding mutants are impaired in the earliest NF responses (7). Several downstream components of the NF signaling cascade, including the leucine-rich-repeat receptor kinase gene *L. japonicus SymRK* (*DMI2*/*NORK* in *Medicago truncatula* and *M. sativa*, respectively) (8, 9), are dually involved in AM and nodulation symbiosis. *SymRK* is likely active near the junction of fungal and rhizobial signaling cascades (8). This makes it a particularly interesting candidate for studying a possible role of legume symbiosis genes in *Casuarina glauca*, which similarly forms AM, but in contrast to legumes interacts not with rhizobia but with *Frankia* bacteria to form actinorhiza.

In actinorhizal symbioses, very little is known about signaling mechanisms involved in plant-bacteria recognition. Analyses of the genome of three *Frankia* strains (10), the biochemical characterization of a *Frankia* root hair-deforming factor whose chemical structure is unknown (11), and the failure of *Frankia* DNA to complement rhizobial *nod* gene mutants (12) suggest that *Frankia* symbiotic signals are structurally different from rhizobial NFs. No plant genes involved in the perception and transduction of *Frankia* symbiotic signals have been identified to date, mostly due to the lack of genetic tools in actinorhiza-forming plants. Here, we isolate *CgSymRK*, a predicted *SymRK* gene from the actinorhizal tree *C. glauca*, and analyze its role in root endosymbioses. Our results reveal that *SymRK* is required for both AM and actinorhiza formation in *C. glauca*, indicating shared genetic mechanisms between fungal and bacterial root endosymbioses in *C. glauca* and legumes.

Results

Isolation of *C. glauca* SymRK. A *C. glauca SymRK* candidate, *CgSymRK*, was isolated by using a degenerate priming approach based on similarity with legume *SymRK* sequences. The gene is 7,280 bp long and contains 15 putative exons, encompassing a 2,829-bp coding sequence. Intron positions and phases are identical to *SymRK* genes of *L. japonicus* and other legumes, including *Medicago truncatula*, *Pisum sativum*, and *Sesbania*
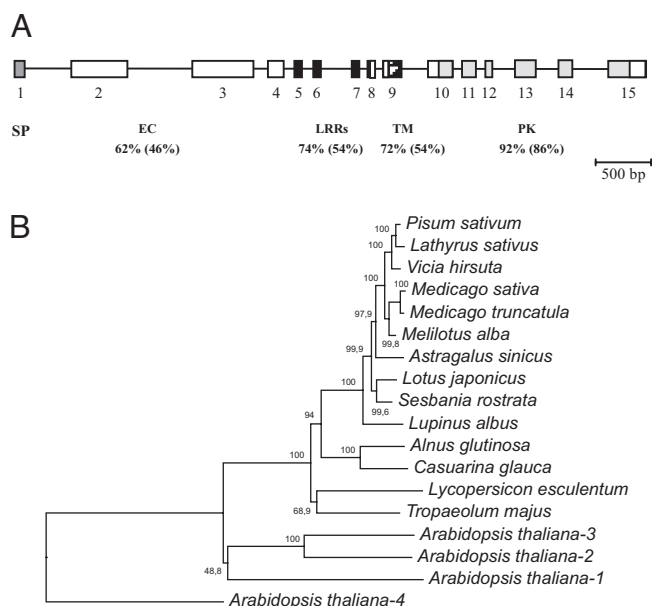

Fig. 1. *C. glauca SymRK* gene. (*A*) Genomic structure of *CgSymRK* with indicated predicted protein domains. Exons are depicted as boxes, introns as a black line. SP, predicted signal peptide; EC, extracellular domain; LRR leucine-rich repeat motifs; TM, transmembrane domain; PK, protein kinase domain. Percentages of similarity and identity between *Cg*SYMRK and *Lj*SYMRK are indicated below each predicted protein domain. (*B*) Distance tree of predicted SYMRK protein sequences based on a CLUSTALW alignement. Numbers above the branches represent the percentages of 1,000 bootstrap replications.

rostrata. The predicted protein of 941 aa contains an N-terminal region of unknown function, three leucine-rich repeat motifs, a transmembrane region, and a serine/threonine protein kinase (Fig. 1*A*). The SYMRK kinase domain is highly conserved between legumes and actinorhizal plants. However, SYMRK extracellular regions are conserved between the two actinorhizal plants *C. glauca* and *A. glutinosa* and highly variable between legumes and actinorhizal plants (data not shown). Both actinorhizal proteins cluster together in a phylogenetic distance tree in the same subgroup as the legume SYMRK (Fig. 1*B*). Southern blot experiments suggested that only one *SymRK* gene exists in *C. glauca* (data not shown). In *C. glauca* roots infected with *Frankia*, real-time expression analysis revealed very little change in *CgSymRK* transcript abundance within 2 weeks after inoculation [supporting information (SI) Fig. 5*A*]. However, we cannot rule out that localized changes in *CgSymrk* expression might occur. *CgSymRK* expression was three times higher in 3-week-old nodules than in uninoculated roots (SI Fig. 5*B*).

CgSymRK Is Necessary for Actinorhizal and AM Symbioses in C. glauca.
To investigate the role of *SymRK* in root endosymbioses in *C. glauca*, we reduced *CgSymRK* expression levels in *Agrobacterium*-induced hairy roots by using RNAi. In parallel, control plants bearing nontransgenic and hairy roots transformed with a control vector comprising the *GFP* reporter gene but lacking the RNAi cassette were analyzed. A total of 78 RNAi composite plants and 48 transgenic control composite plants showing high GFP fluorescence in hairy roots were analyzed in two independent experiments. At 3 weeks after inoculation, plants transformed with the control vector began to develop nodules that were similar in size and shape to those produced on nontransgenic roots (Fig. 2 *A* and *B*). As observed in ref. 13, nodulation of transgenic control hairy roots was reduced compared with nontransgenic controls. In *CgSymRK* RNAi roots, the frequency of nodulated root systems was 50% less than in transgenic control root systems (SI Table 1). Nodulated
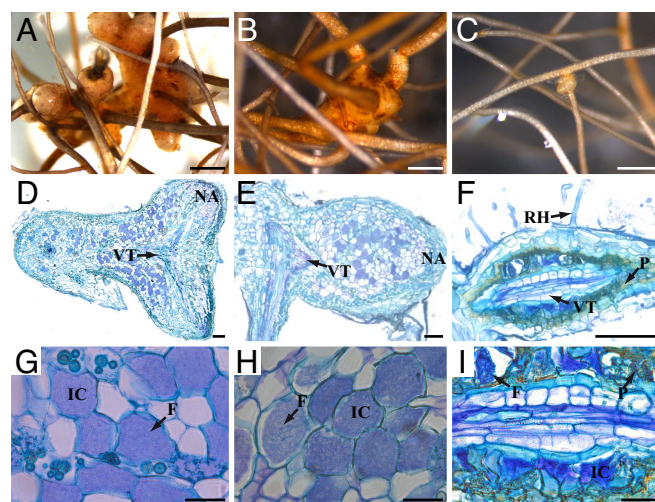

Fig. 2. Knockdown phenotype of *CgSymRK* after *Frankia* inoculation. (*A*) Nontransgenic nodule consisting of multiple lobes 10 weeks postinoculation (wpi). A nodular root develops at the apex of each nodule lobe. (*B*) Nodule on a hairy root transformed with a control vector at 10 wpi. Nodule morphology is similar to wild-type nodules. (*C*) Nodule-like structure formed on *CgSymRK* knockdown (RNAi) roots 10 wpi. Nodule lobes are small and do not branch to form a multilobed structure. (*D* and *E*) Sections of wild-type and transgenic control nodules. Each nodule lobe exhibits a central vascular bundle and cortical parenchyma infected with *Frankia*. (*F*) Section of a nodule-like structure observed on an RNAi plant showing few small infected cells and abnormal accumulation of polyphenols in the endodermis. (*G*) Closeup of area in *D*, showing both infected and uninfected cortical cells. Infected cells are hypertrophied and filled with *Frankia*. (*H*) Closeup of area in *E*. As in nontransgenic nodules, hypertrophied cortical cells are filled with *Frankia*. (*I*) Closeup of area in *F*. Infected cells are few and small compared with cells in nontransgenic and transgenic control nodules. IC, infected cell with *Frankia*; RN, root nodule; NA, nodule apex; VT, vascular tissue; P, polyphenol droplets; RH, root hair. [Scale bars: 1 mm (*A*–*C*); 100 μm (*D*–*F*); 25 μm (*G*–*I*).]

RNAi roots showed strong alterations in nodule development compared with control roots. We observed a gradient of phenotypes ranging from aborted prenodules (Fig. 2 *C* and *F*) to nodules usually consisting of one thin lobe, whereas mature nodules in transgenic and nontransgenic control roots were multilobed (Fig. 2 *A* and *B* and *D* and *E*). On *CgSymRK* RNAi root nodules, the nodular roots, which are unbranched roots exhibiting negative geotropism growing at the apex of each nodule lobe, often behaved like adventitious roots exhibiting normal root growth and branching (data not shown). These aberrant nodules and nodular roots were never seen on transgenic or nontransgenic control roots. Histological analysis of 10 aberrant symbiotic structures of *CgSymRK* RNAi roots revealed an accumulation of phenolic compounds (Fig. 2*F*) and the presence of small infected cells in the cortex (Fig. 2*I*) contrasting with the hypertrophied infected cells observed in nontransgenic and transgenic control nodules (Fig. 2 *G* and *H*). We tested the ability of *CgSymRK* RNAi nodules to fix nitrogen via acetylene reduction activity (ARA) assays. *CgSymRK* RNAi nodules exhibited a quasinull ARA compared with transgenic control nodules (SI Fig. 6). To test the efficacy of *CgSymRK* knockdown in RNAi roots, *CgSymRK* expression was tested by quantitative RT-PCR (qPCR) in subcultivates of five *CgSymRK* RNAi roots. A 52–76% reduction of *CgSymRK* mRNA levels was observed in RNAi roots compared with transgenic control roots (SI Fig. 7). Taken together, our results indicate that a reduction in *CgSymRK* expression results in severe impairment in actinorhiza formation and symbiotic nitrogen fixation.

In legumes, *SymRK* has been shown to play also a crucial role in the establishment of AM symbiosis (14). To investigate whether *CgSymRK* is also involved in AM formation in *C. glauca*,

RNAi hairy roots plants were generated and cultivated in pots containing *Glomus intraradices* inoculum. Plants were harvested after 4 or 8 weeks, and GFP fluorescence was checked in transformed roots. Seventeen control and 21 RNAi plants showing GFP fluorescence and six nontransformed root systems were subjected to AM analysis. In nontransgenic control plants, fungal structures such as intraradical hyphae, vesicles, and arbuscules (SI Figs. 8 and 9 *A* and *B*) were observed at high frequencies ranging from 22% to 52% total root length colonization. Similar structures were observed at relatively high frequencies in roots of most transgenic control plants, 4 or 8 weeks after inoculation (SI Figs. 8 and 9 *C* and *D*). The slight reduction of colonization compared with nontransgenic control roots might be linked to modifications of hormonal balance. In contrast, most plants transformed with the *CgSymRK* RNAi construct showed very weak levels of AM colonization, and four composite plants showed a complete absence of intraradical structures 4 weeks after inoculation (SI Fig. 8). The absence of intracellular colonization was not due to an absence of inoculum, because extraradical hyphae were very often observed. Some RNAi roots showed extensive development of extraradical mycelium, usually growing along the epidermal cells and forming appressoria, which were frequently associated with abnormal, swollen hyphal structures (SI Fig. 9 *E* and *F*). Most fungal penetration attempts aborted, resulting in very low levels of intraradical colonization (SI Fig. 8). However, on the rare occasions where penetration succeeded, intraradical hyphae, arbuscules, and vesicles morphologically similar to those found in transgenic and nontransgenic control roots were observed (SI Fig. 9 *G* and *H*). Compared with control roots, colonized patches were generally smaller, spreading over few cells near the entry point and never succeeding in colonizing the whole root. These results indicate that *CgSymRK* knockdown strongly affects early steps of the AM interaction, especially fungal penetration into the root cortex, thereby revealing a conservation of *SymRK* function in AM between legumes and *C. glauca*.

CgSymRK Can Restore Root Endosymbioses in a Legume *symrk* Mutant.

To test whether *CgSymRK* can function in root endosymbioses in a legume, we introduced its coding sequence linked to the *L. japonicus SymRK* promoter region into *Agrobacterium rhizogenes*-induced roots of *L. japonicus symrk-10* (15) mutants. Interaction with AM fungi is usually aborted in *L. japonicus symrk* mutants at the epidermal level (14), with few hyphae invading the root cortex and no arbuscules developing within 3–6 weeks of exposure to fungal inoculum.

Similarly, after 3 weeks of cocultivation with *G. intraradices*, *symrk-10* roots transformed with a vector lacking a *SymRK* expression cassette (control vector) formed no AM, and typical hyphal swellings formed in epidermal cells indicating abortion of fungal infections (SI Table 2; Fig. 3 *A* and *B*). In contrast, wild-type (Fig. 3 *C* and *D*) and *symrk-10* (Fig. 3 *E* and *F*) plants transformed with *CgSymRK* developed AM (SI Table 2), involving the formation of wild-type-like cortical arbuscules (Fig. 3*F*) and infection sites in the complemented mutants. Similar results were obtained with wild-type and *symrk-10* mutant plants transformed with an *LjSymRK* expression cassette controlled by the same promoter region (SI Table 2). These results demonstrate that *CgSymRK* can complement the mycorrhization defect of *L. japonicus symrk* mutants.

Wild-type *L. japonicus* plants respond to inoculation with their rhizobial symbiont *Mesorhizobium loti* by root hair curling, infection thread formation, and nodule development. *L. japonicus symrk* mutants, in contrast, show no normal curling reaction of root hairs, and bacteria are unable to induce infection thread or nodule formation (8). This was equally the case in *symrk-10* roots transformed with a control vector (SI Table 2; Fig. 4 *A* and *B*), whereas *L. japonicus* wild-type and *symrk-10* roots carrying *CgSymRK* formed wild-type-like infection threads and nodules (Table 2; Fig.
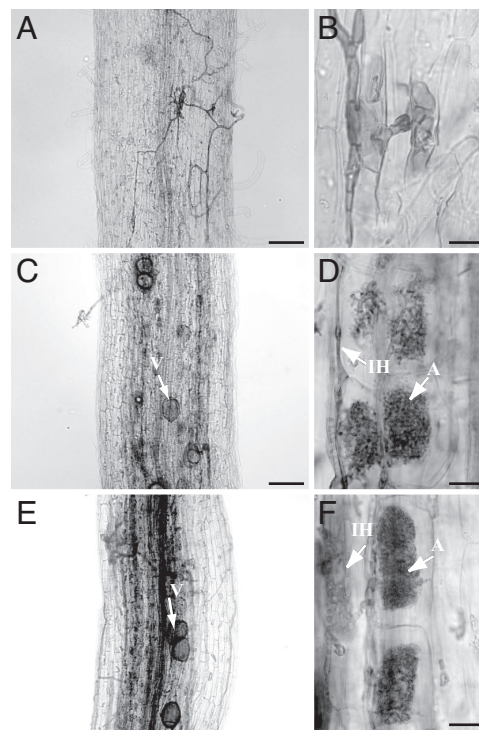

Fig. 3. AM formation in *L. japonicus symrk-10* mutants complemented with the *CgSymRK* coding sequence under control of the *LjSymRK* promoter, after 3 weeks of cocultivation with *G. intraradices*. Cleared roots with fungal structures are stained with acidic ink. (*A* and *B*) *symrk-10* roots transformed with a control vector. (*A*) Noncolonized root with extraradical mycelium and aborted infection structure (arrow). (*B*) Fungal appressorium and entry point associated with aborted infection structure within host epidermal cell. (*C* and *D*) Wild-type and (*E* and *F*) *symrk-10* roots transformed with *CgSymRK* linked to the *LjSymRK* promoter. Fungal hyphae grow through epidermis and exodermis and form arbuscules and vesicles in the inner root cortex. A, arbuscule; IH, intraradical hyphae; V, vesicle. [Scale bars: 100 μm (*A*, *C*, and *E*); 20 μm (*B*, *D*, and *F*).]

4 *C–E* and *F-H*, respectively). These exhibited bacteria-filled and noninfected host cells (Fig. 4 *I* and *J*). *L. japonicus* wild-type and *symrk-10* roots transformed with a *L. japonicus SymRK* expression cassette equally formed infection threads and infected nodules (SI Table 2; Fig. 4 *K* and *L*, respectively). The observation that *SymRK* from the actinorhiza-forming plant *C. glauca* can restore not only the interaction with AM fungi but also with *M. loti* bacteria in *L. japonicus symrk* mutants indicates that this gene is highly conserved in its function in both AM and nodulation symbioses, whereas the specificity of recognition of bacterial partners is *SymRK*-independent.

Discussion

There are three major types of root endosymbioses in angiosperms. These include the arbuscular mycorrhiza symbiosis with fungi and nitrogen-fixing root nodulation of legumes and actinorhiza-forming plants. In recent years, there has been a tremendous increase in knowledge of the molecular mechanisms responsible for NF perception and signal transduction in legumes (6). Genetic approaches in model legumes led to the identification of several components and the definition of a signaling cascade (5). Part of this signaling cascade is also involved in transduction of the symbiotic signal in AM symbioses (5). This gave rise to the hypothesis that the evolutionarily recent legume–rhizobia symbiosis reuses some of the molecular mechanisms of the more ancient AM symbiosis (16). This common signaling pathway includes the receptor kinase *SymRK*/*DMI2*. So far, nothing is known about the symbiotic signals and their perception during actinorhizal symbioses. Available data
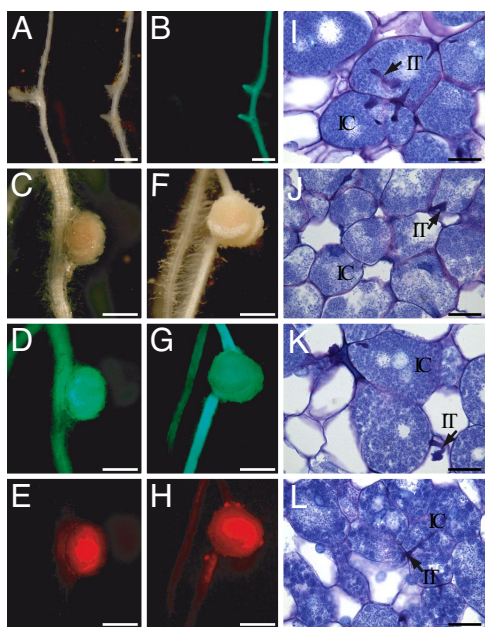
Fig. 4. Nodulation in *L. japonicus symrk-10* mutants complemented with the *CgSymRK* coding sequence under control of the *LjSymRK* promoter, 8 weeks after inoculation with *M. loti* MAFF expressing *DsReD*. Transgenic roots carried an *sGFP* reporter gene. (*A*, *C*, and *F*) Roots and nodules under white light. (*B*, *D*, and *G*) Transgenic roots and nodules showing GFP fluorescence. (*E* and *H*) Red fluorescence of bacterial DsRED. (*A* and *B*) *symrk-10* root transformed with the control vector, showing no nodules. (*C–E*) Transgenic wild-type root carrying the *Cg-SymRK* coding sequence. Nodules contain *DsReD*-expressing bacteria (*E*). (*F–H*) *symrk-10* mutant root transformed with the *CgSymRK* coding sequence, carrying wild-type-like nodules. (*I–L*) Semithin sections of nodules stained with toluidine blue. (*I* and *J*) Nodules on *symrk-10* mutant and wild-type roots complemented with the *CgSymRK* coding sequence, respectively. (*K* and *L*) Nodules on *symrk-10* mutant and wild-type roots complemented with the *LjSymRK* coding sequence, respectively. Infection threads (IT) are contained within bacteria-infected cells (IC). [Scale bars: 500 μm (*A–H*); 25 μm (*I–L*).]

indicate only that the *Frankia* symbiotic signal is likely chemically different from NFs (10–12). Here, we report the isolation and characterization of *CgSymRK*, a *SymRK*/*DMI2* homolog from the actinorhizal tree *C. glauca*. Our data demonstrate that *CgSymRK* is functionally equivalent to *LjSymRK* in symbiosis formation in *L. japonicus*. In our experience, both AM and nodulation symbiosis formation in hairy roots of *L. japonicus* can vary in efficiency, particularly in complemented mutant tissue. Despite the differences in numbers of rescued root systems between the symbiosis types (*CgSymRK*) and constructs, phenotypic analyses clearly suggest that both symbiosis types can be fully supported by *CgSymRK* in *L. japonicus*.

Moreover, we were able to show that *CgSymRK* is necessary for functional symbiosis with *Frankia*. We therefore conclude that *CgSymRK* is probably a component of the signaling pathway involved in the perception and the transduction of yet-unknown *Frankia* factors. As in legumes (17, 18) *CgSymRK* expression level remained constant during root infection and increased in mature nodules compared with noninoculated roots. The reduction in the number of nodulated plants obtained by RNAi is less pronounced than the one obtained in legumes (18, 19); however, it clearly indicates that *CgSymRK* is involved during the early stages of *Frankia* root hair infection. A second symbiotic defect was observed downstream of this infection with striking differences in the nodule morphology and tissue organization relative to the control. *Cg-SymRK* RNAi hairy roots mostly developed small nonfixing nodule-like structures. Light microscopy revealed that the nodule apical

meristem was absent, and we did not observe the gradient of infection and differentiation in the cortex that is present in transgenic and nontransgenic control nodules. Cortical cells also seemed to be less infected, and infected cells were smaller than those of control nodules. In addition, we observed the formation of dense deposits of polyphenols in *CgSymRK* RNAi nodules. These data suggest that the loss of *CgSymRK* function also affects *C. glauca–Frankia* symbiotic interaction after bacterial penetration. This is consistent with qPCR results that indicate an enhancement of *CgSymRK* expression in mature nodules.

We also analyzed the role of *CgSymRK* in the *G. intraradices–C. glauca* interaction. Hairy roots of *C. glauca* carrying the *CgSymRK* RNAi construct were able to form arbuscules and vesicles morphologically similar to those found in control plants, suggesting that *CgSymRK* is not involved in the formation of these late symbiotic structures. However, most RNAi plants showed a significant decrease in fungal colonization. At the root surface, hyphae developed abundant appressoria, but these colonization attempts rarely succeeded, pointing to a role of *CgSymRK* during hyphal penetration. Similar results were shown for *L. japonicus symrk* (14) and *M. truncatula dmi2* mutants (20, 21). This work report a role of *SymRK* in AM symbiosis formation in a nonlegume plant.

In summary, our data indicate that *SymRK* is involved in the symbiotic signal transduction pathway leading to actinorhizal symbioses. Our results demonstrate that, in *C. glauca* as in legumes, *SymRK* is involved in the establishment of both nitrogen-fixing nodule and AM symbioses, thus supporting the hypothesis that signaling genes have been recruited from the more ancient AM symbiosis during the evolution of nitrogen-fixing symbioses. It will now be essential to compare signal transduction pathways involved in endosymbiotic accommodation of AM fungi, rhizobia, and *Frankia* to develop strategies for the transfer of nodulation to nonnodulated plants.

Materials and Methods

Plant, Bacterial, and Fungal Material. *C. glauca* seeds were provided by Carter Seeds and grown as described in ref. 22. *L. japonicus* ecotype B-129 Gifu and *L. japonicus symrk* mutant *symrk-10* from the same ecotype (15) were grown for transformation as described in ref. 23. *C. glauca* and *L. japonicus* plants were transformed with *A. rhizogenes* strains A4RS (24) and AR1193 (25). For nodulation phenotyping of *C. glauca*, plants were inoculated with *Frankia* strain CcI3. *C. glauca* mycorrhization experiments were performed in pots containing an autoclaved mixture of quartz sand and soil (4:1). Plants were transferred from *in vitro* cultures and grown for 4–8 weeks in a growth chamber and watered with a modified Hoagland solution (22) containing 10 μM phosphate. *G. intraradices* inoculum was prepared by extracting spores from *in vitro* cultures of *G. intraradices* (26). One Petri dish showing extensive sporulation was kept at 4°C for at least 3 weeks and used to inoculate 2 liters of sand:soil mixture. For nodulation phenotyping of *L. japonicus*, composite plants were grown in plastic pots with 300 ml of Seramis substrate (Mars) and 150 ml of FP medium (27) and inoculated with *Mesorhizobium loti* strain MAFF expressing *DsReD* (M. Hayashi, personal communication). To test for AM formation, plants were cocultivated with *G. intraradices* BEG195 in chive nurse pots as described (14) and harvested after 3 weeks. Transgenic roots were selected via GFP fluorescence and stained with acidic ink as described (14) for visualization of fungal structures.

Identification and Cloning of *CgSymRK* Sequences and Phylogenetic Analysis. Amplification of *CgSymRK* was conducted on a cDNA library prepared from *C. glauca* uninfected roots by using the degenerated primers *SymRKdeg-5* (5′-CCAAGACATGAATGGTCTCTGGTNGARTGGGC-3′) and *SymRKdeg-3* (5′-GAATC-CATAGATCTCATATATTCAGAAGCRTTRTTYTC-3′). The amplified fragment was cloned into a pGEM-T easy vector (Promega) and sequenced. cDNA fragments were obtained by RACE-PCR on a root cDNA library by using the Marathon cDNA amplification kit (Clontech), and the CDS was amplified by using primers *CgSymRKATG* (5′-ATGATGGAGGGATTGCATAAT-3′) and *CgSymRKSTOP* (5′-TCCTCCACAGCCAAGATAA -3′). The *CgSymRK* genomic sequence was obtained by using a Genome Walker kit (Clontech) and cloned in a pGEM-T easy vector. For the phylogenetic analysis, sequences (with GenBank accession numbers in parentheses) from *Alnus glutinosa* (62946487), *Sesbania rostrata* (56412259), *Melilotus alba* (21698802), *Pisum sativum* (21698794), *Lathyrus sativus* (89213719), *Vicia hirsuta* (21698800), *Medicago truncatula* (21698783), *Lotus japonicus*

(21622628), *Medicago sativa* (21698781), *Lupinus albus* (62946493), *Tropaeolum majus* (62946489), *Astragalus sinicus* (61723807), and *Lycopersicon esculentum* (62944413) were retrieved from GenBank via BLASTP search performed with the *L. japonicus*-predicted SYMRK sequence. Sequences of SYMRK homologs in *Arabidopsis thaliana* (−: At5g48740; −2: At2g37050; −3 At1g67720) described in ref. 28 were also included. *A. thaliana* (−: At3g25560), an NSP-interacting kinase (29), was used to root the tree. The alignment was performed by using the CLUSTALW and Neighbor-Joining algorithms in the CLC-Free Workbench 4 software package (CLC bio).

***Agrobacterium rhizogenes*-Mediated Transformation, RNAi and Complementation.** *C. glauca* and *L. japonicus* hairy root transformation was performed by following standard procedures (13, 23). To produce the knockdown construct, 365 bp corresponding to the kinase domain of *CgSymRK* sequence were amplified from genomic DNA by using *CgRNAi*-5 (5′-GGGAGCTGGAGGAT-GCTTTGA-3′) and *CgRNAi*-3 (5′-TAAGTAGTAGTAGGTGGGGAGATTATTC-3′) primers containing 5′ XhoI or BamHI restriction sites for *CgRNAI-5* and KpnI or ClaI for *CgRNAI-3*. Amplified fragments (XhoI-*CgRNAi*-KpnI and BamHI-*CgRNAi*-ClaI) were then cloned into pKannibal (30) downstream of the CaMV 35S promoter, and the RNAi cassette was then cloned into the pHKN29 binary vector (31). This vector also contains the GFP gene under the control of the CaMV 35S promoter. For functional complementation, the *CgSymRK* coding sequence was fused to *LjSymRK* promoter (2,415-bp) and terminator (315-bp) regions and transferred into the pHKN29 binary vector. For complementation of *L. japonicus symrk* mutants with *LjSymRK*, the binary vector pCAMBIA 1302 was equipped with 4,970 bp of the *LjSymRK* promoter region fused to the *LjSymRK* coding sequence and a 285-bp NOS terminator fragment amplified from pJawohl8 RNAi [kind gift of P. Schulze-Lefert (Max Planck Institute, Cologne, Germany)] by using primers TNOS-5 5′-AATAAACCTAGGATCAGCT-TGCATGCCGGTCG-3′ and TNOS-3 5′-AAATAAGTCGACCTAGAGTCAAGCA-GATCGTTCAAAC-3′.

qPCR and Acetylene Reduction Assay. Total RNA was extracted by using the RNeasy Plant Mini Kit (Qiagen). RNAs were quantified with Quant-iT Ribogreen RNA Reagent (Invitrogen). One hundred nanograms of total RNA was reverse-transcribed by using SuperScriptIII H⁻ reverse transcriptase (Invitrogen) and oligo(dT)$_{12-18}$. qPCR was performed by using the FullVelocity SYBR Green QPCR Master Mix (Stratagene). The primers used were *qCgSymRKFor1* 5′-GCAGGAGGTAGCAGTGAAGGTTC-3′ and *qCgSymRKRev2* 5′-GCGATCTTGAAGCGAGCCATTAG-3′. The FullVelocity cycling PCR program on an MX 3005P (Stratagene) was as follows: 1 cycle at 95°C for 5 min, 40 cycles at 95°C for 10 s and 60°C for 30 s, ended by 1 cycle at 95°C for 1 min, 60°C for 30 s, and 95°C for 30 s. Reactions were performed in triplicate, and the comparative threshold-cycle method was used to quantify *CgSymRK* expression (32). The results were standardized with *CgUbi* expression levels (32). The acetylene reduction assay was performed according to ref. 33.

Histochemical Analysis and Microscopy. *C. glauca* nodules were fixed as described in ref. 34. *L. japonicus* nodules were fixed in a solution containing 50% EtOH, 4% formaldehyde, and 5% acetic acid and dehydrated in 70% EtOH. Samples were embedded in Technovit 7100 resin (Heraeus Kulzer), and thin sections (6 μm) were cut with a microtome (Microm HM355S), stained with toluidine blue (0.01%), and mounted in Clearium Mountant (Surgipath). Visualization of AM in *L. japonicus* was performed as described in ref. 14. To visualize AM in *C. glauca*, roots were cleared for 1–2 days in 10% KOH at 90°C, rinsed, and stained for at least 1 h with a 0.05% trypan blue/5% acetic acid solution at 60°C and destained in water as described (35). Samples were viewed under a DMRB microscope (Leica). Colonization was assessed with a microscope by using the gridline intersect method (35) on at least 100 intersections per sample.

1. Schüssler A, Schwarzott D, Walker C (2001) A new fungal phylum, the *Glomeromycota*: phylogeny and evolution. *Mycol Res* 105:1413–1421.
2. Soltis DE, *et al*. (1995) Chloroplast gene sequence data suggest a single origin of the predisposition for symbiotic nitrogen fixation in angiosperms. *Proc Natl Acad Sci USA* 92:2647–2651.
3. Pawlowski K, Bisseling T (1996) Rhizobial and actinorhizal symbioses: What are the shared features? *Plant Cell* 8:1899–1913.
4. D'Haeze W, Holsters M (2002) Nod factor structures, responses, and perception during initiation of nodule development. *Glycobiology* 12:79R–105R.
5. Oldroyd GE, Downie JA (2006) Nuclear calcium changes at the core of symbiosis signalling. *Curr Opin Plant Biol* 9:351–357.
6. Jones KM, Kobayashi H, Davies BW, Taga ME, Walker GC (2007) How rhizobial symbionts invade plants: the *Sinorhizobium-Medicago* model. *Nat Rev Microbiol* 5:619–633.
7. Radutoiu S, *et al*. (2003) Plant recognition of symbiotic bacteria requires two LysM receptor-like kinases. *Nature* 425:585–592.
8. Stracke S, *et al*. (2002) A plant receptor-like kinase required for both bacterial and fungal symbiosis. *Nature* 417:959–962.
9. Endre G, *et al*. (2002) A receptor kinase gene regulating symbiotic nodule development. *Nature* 417:962–966.
10. Normand P, *et al*. (2007) Genome characteristics of facultatively symbiotic *Frankia* sp. strains reflect host range and host plant biogeography. *Genome Res* 17:7–15.
11. Ceremonie H, Debelle F, Fernandez MP (1999) Structural and functional comparison of *Frankia* root hair deforming factor and rhizobia Nod factor. *Can J Bot* 77:1293–1301.
12. Ceremonie H, Cournoyer B, Maillet F, Normand P, Fernandez MP (1998) Genetic complementation of rhizobial nod mutants with *Frankia* DNA: artifact or reality? *Mol Gen Genet* 260:115–119.
13. Diouf D, *et al*. (1995) Hairy root nodulation of *Casuarina glauca*: a system for the study of symbiotic gene expression in actinorhizal tree. *Mol Plant–Microb Interact* 8:532–537.
14. Demchenko K, Winzer T, Stougaard J, Parniske M, Pawlowski K (2004) Distinct roles of *Lotus japonicus* SYMRK and SYM 15 in root colonization and arbuscule formation. *New Phytol* 163:381–392.
15. Perry JA, *et al*. (2003) A TILLING reverse genetics tool and a web-accessible collection of mutants of the legume *Lotus japonicus*. *Plant Physiol* 131:866–871.
16. Kistner C, Parniske M (2002) Evolution of signal transduction in intracellular symbiosis. *Trends Plants Sci* 7:511–518.
17. Bersoult A, *et al*. (2005) Expression of the *Medicago truncatula* DM12 gene suggests roles of the symbiotic nodulation receptor kinase in nodules and during early nodule development. *Mol Plant–Microbe Interact* 18:869–876.
18. Capoen W, Goormachtig S, De Rycke R, Schroeyers K, Holsters M (2005) SrSymRK, a plant receptor essential for symbiosome formation. *Proc Natl Acad Sci USA* 102:10369–10374.
19. Limpens E, *et al*. (2005) Formation of organelle-like N2-fixing symbiosomes in legume root nodules is controlled by *DMI2*. *Proc Natl Acad Sci USA* 102:10375–10380.
20. Morandi D, Prado E, Sagan M, Duc G (2005) Characterisation of new symbiotic *Medicago truncatula* (Gaertn.) mutants, and phenotypic or genotypic complementary information on previously described mutants. *Mycorrhiza* 15:283–289.
21. Calantzis C, Morandi D, Arnould C, Gianinazzi-Pearson V (2001) Cellular interactions between *G. mosseae* and a Myc(-) *dmi2* mutant in *Medicago truncatula*. *Symbiosis* 30:97–108.
22. Franche C, *et al*. (1997) Genetic transformation of the actinorhizal tree *Allocasuarina verticillata* by *Agrobacterium tumefaciens*. *Plant J* 11:897–904.
23. Diaz G, Gronlund M (2005) in *Lotus japonicus Handbook*, ed Marquez AJ (Springer, New York), pp 261–277.
24. Jouanin L, Tourneur J, Tourneur C, Casse-Delbart F (1986) Restriction maps and homologies of the three plasmids of *Agrobacterium rhizogenes* strain A4. *Plasmid* 16:124–134.
25. Stougaard J, Abildsten D, Marcker KA (1987) The *Agrobacterium rhizogenes* pRi TL-DNA segment as a gene vector system for transformation of plants. *Mol Gen Genet* 207:251–255.
26. St-Arnaud M, Hamel C, Vimard B, Caron M, Fortin JA (1996) Enhanced hyphal growth and spore production of the arbuscular mycorrhizal fungus *Glomus intraradices* in an *in vitro* system in the absence of host roots. *Mycol Res* 100:328–332.
27. Fahraeus G (1957) The infection of clover root hairs by nodule bacteria studied by a simple glass slide technique. *J Gen Microbiol* 16:374–381.
28. Zhu H, Riely BK, Burns NJ, Ane JM (2006) Tracing nonlegume orthologs of legume genes required for nodulation and arbuscular mycorrhizal symbioses. *Genetics* 172:2491–2499.
29. Fontes EPB, Santos AA, Luz DF, Waclawovsky AJ, Chory J (2004) The geminivirus nuclear shuttle protein is a virulence factor that suppresses transmembrane receptor kinase activity. *Genes Dev* 18:2545–2556.
30. Wesley SV, *et al*. (2001) Construct design for efficient, effective and high-throughput gene silencing in plants. *Plant J* 27:581–590.
31. Kumagai H, Kouchi H (2003) Gene silencing by expression of hairpin RNA in *Lotus japonicus* roots and root nodules. *Mol Plant–Microbe Interact* 16:663–668.
32. Hocher V, *et al*. (2006) Expressed sequence-tag analysis in *Casuarina glauca* actinorhizal nodule and root. *New Phytol* 169:681–688.
33. Hardy RW, Holsten RD, Jackson EK, Burns RC (1968) The Acetylene-Ethylene Assay for N (2) Fixation: Laboratory and Field Evaluation. *Plant Physiol* 43:1185–1207.
34. Svistoonoff S, *et al*. (2003) cg12 expression is specifically linked to infection of root hairs and cortical cells during *Casuarina glauca* and *Allocasuarina verticillata* actinorhizal nodule development. *Mol Plant–Microbe Interact* 16:600–607.
35. Brundrett MC, Piché Y, Peterson RL (1984) A new method for observing the morphology of vesicular-arbuscular mycorrhizae. *Can J Bot* 62:2128–2134.